

Simultaneous Shape Reconstruction and Force Estimation of Soft Bending Actuators Using Distributed Inductive Curvature Sensor

Yu Mei¹, Lei Peng¹, Hongyang Shi², Xinda Qi¹, Yiming Deng¹, Vaibhav Srivastava¹
and Xiaobo Tan¹

¹ Department of Electrical and Computer Engineering
Michigan State University

² Department of Electrical and Computer Engineering
The University of Texas at Austin

July 17, 2024

AIM 2024

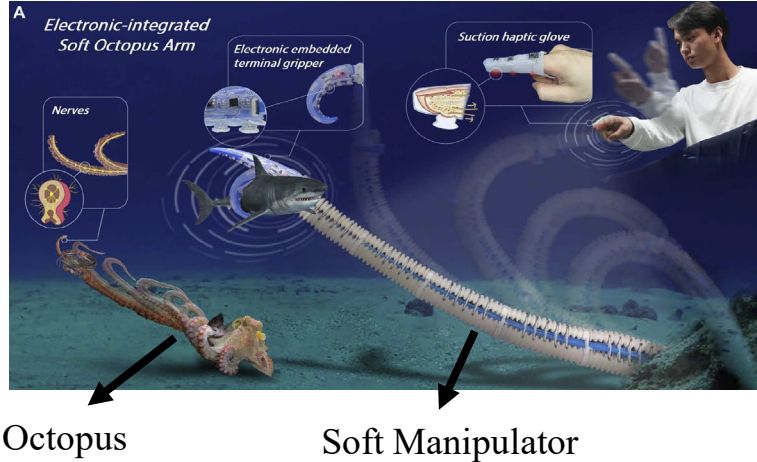


Background of Soft Robots

Research Trend

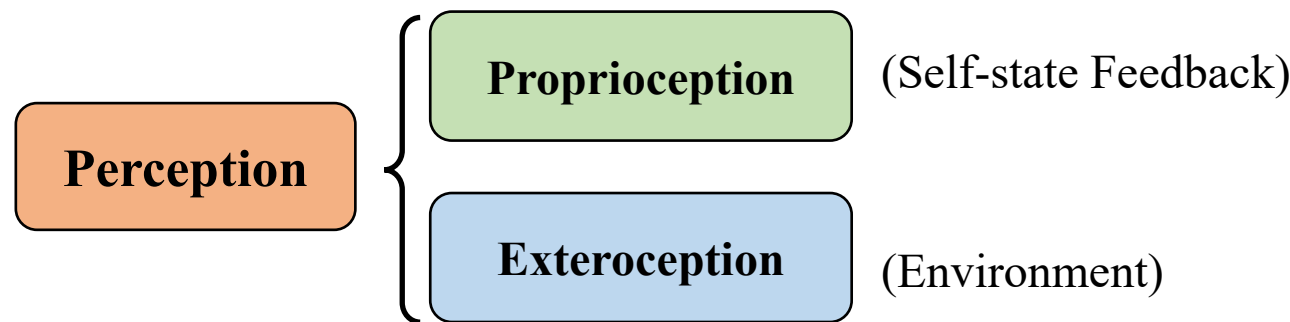
Equip soft robots with **biological intelligence** to interact with the environment.

Examples ¹



Octopus

Soft Manipulator



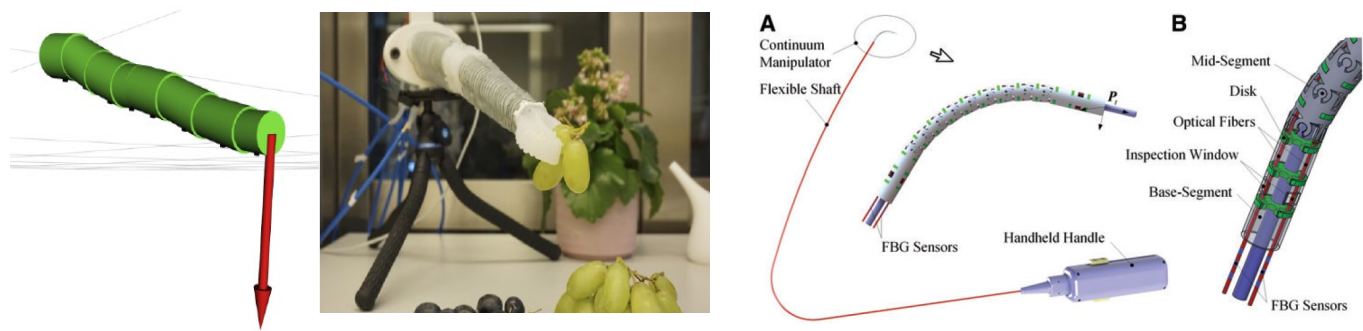
¹ Z. Xie et al., "Octopus-inspired sensorized soft arm for environmental interaction," *Science Robotics*, 2023.

Perception System of Soft Robots

Challenges

- ❑ Flexible and Stretchable
- ❑ Infinite degrees of freedom
- ❑ Undesired external sensors

Related Work²⁻³



Goal

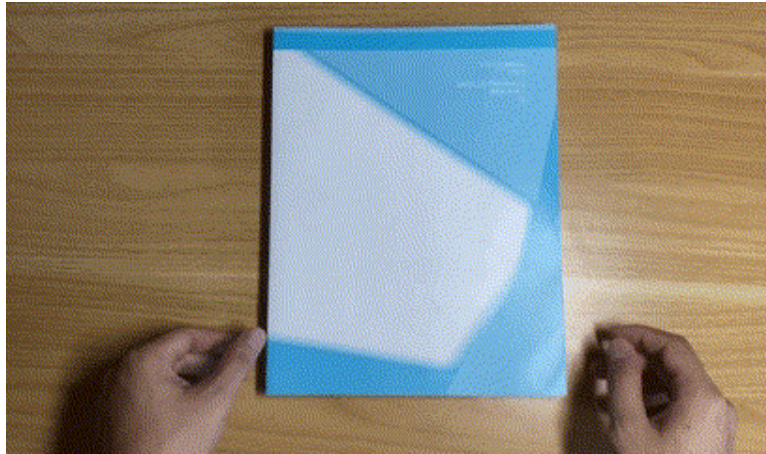
Simultaneous high-resolution shape sensing and accurate external force estimation using only a proprioceptive sensor.

² Y. Toshimitsu, K. W. Wong, T. Buchner, and R. Katzschmann, “SoPrA: Fabrication amp; Dynamical Modeling of a Scalable Soft Continuum Robotic Arm with Integrated Proprioceptive Sensing,” in *2021 IEEE/RSJ International Conference on Intelligent Robots and Systems (IROS)*.

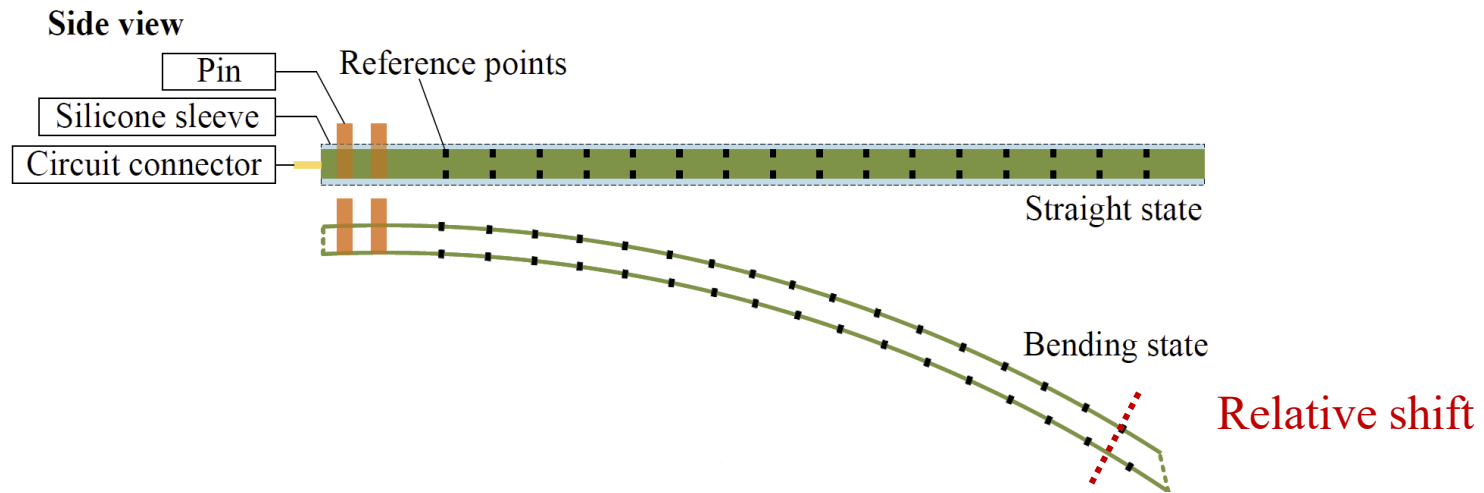
³ A. Gao, N. Liu, M. Shen, M. E.M.K. Abdelaziz, B. Temelkuran, and G.-Z. Yang, “Laser-Profiled Continuum Robot with Integrated Tension Sensing for Simultaneous Shape and Tip Force Estimation,” *Soft Robotics*, vol. 7, no. 4, pp. 421–443, Aug. 2020.

Sensor Concept

□ Sensor principle



□ Proposed shape sensor



Distributed Inductive Curvature Sensor

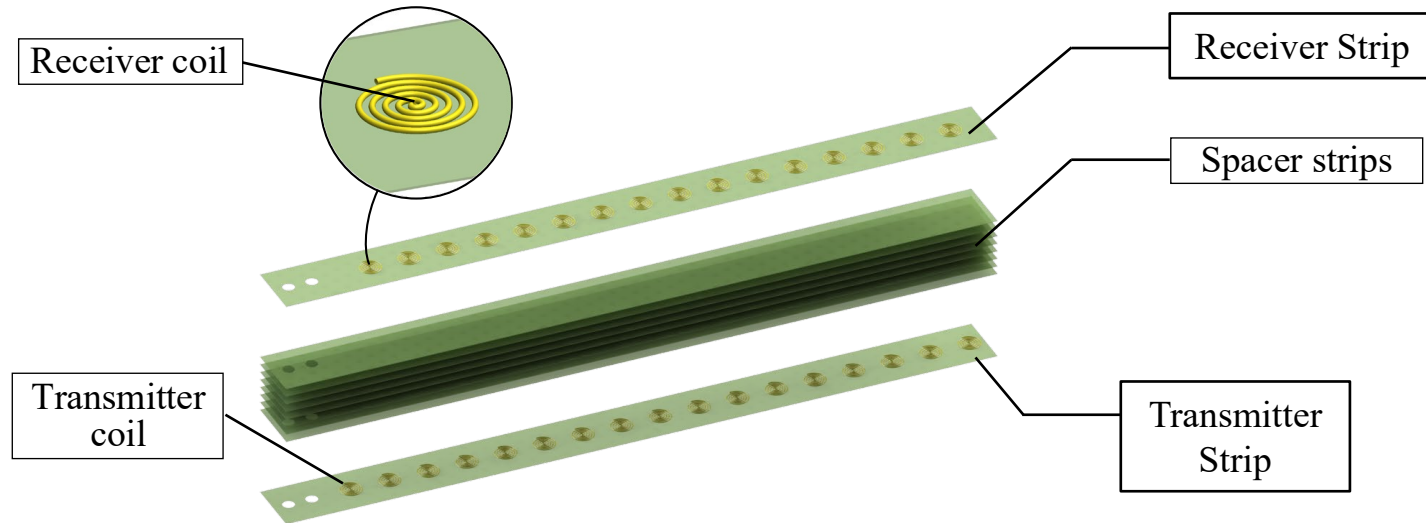
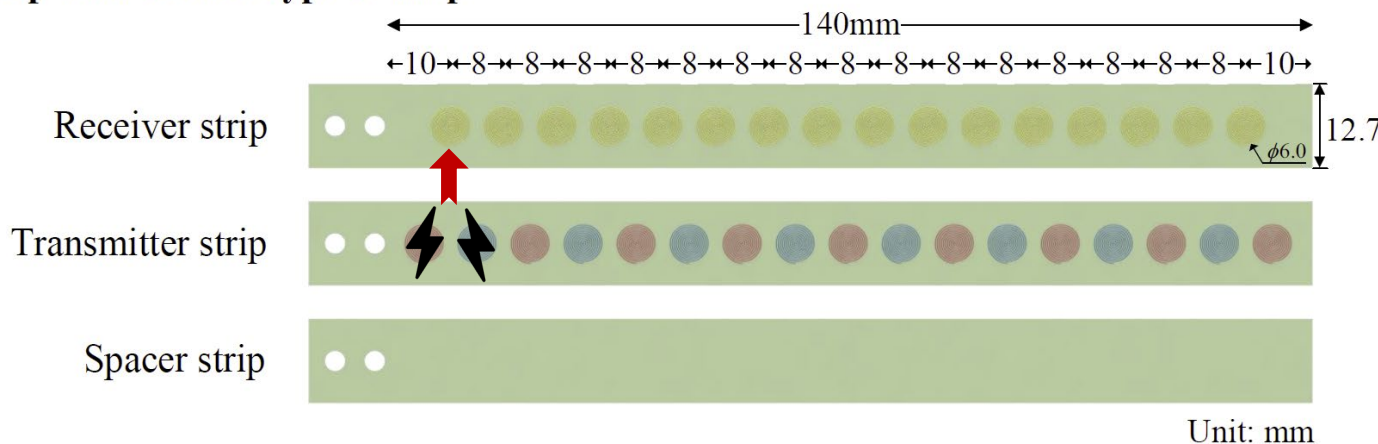


Figure: Sensor structure

Top view of each type of strip



Distributed Inductive Curvature Sensor



Figure: Sensor Prototype

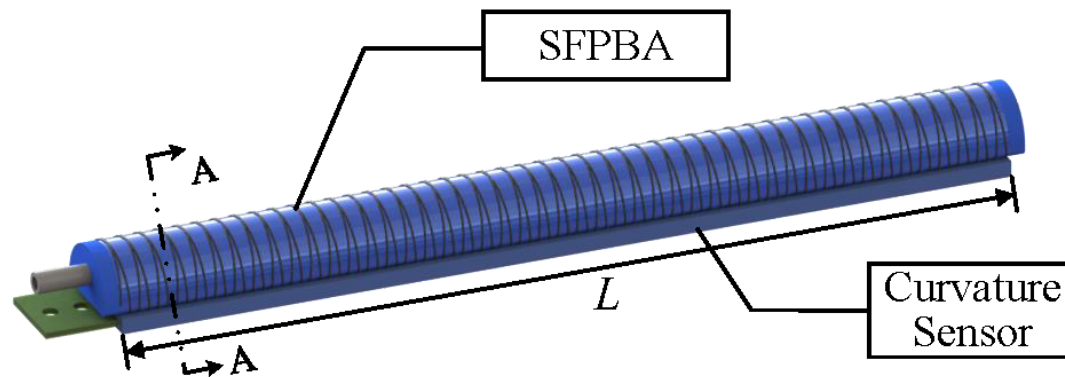
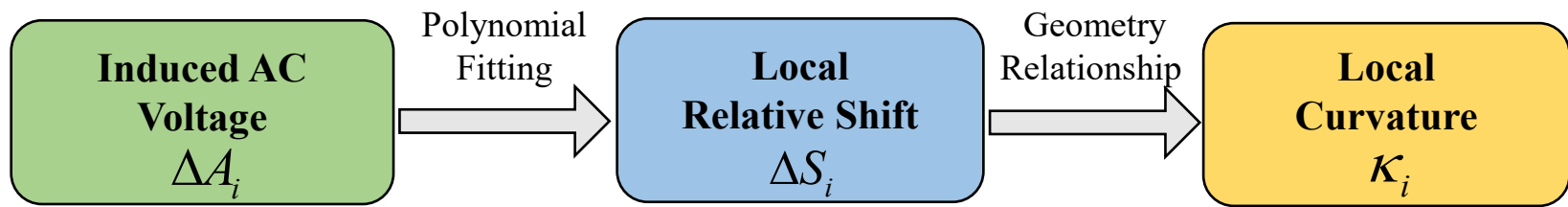
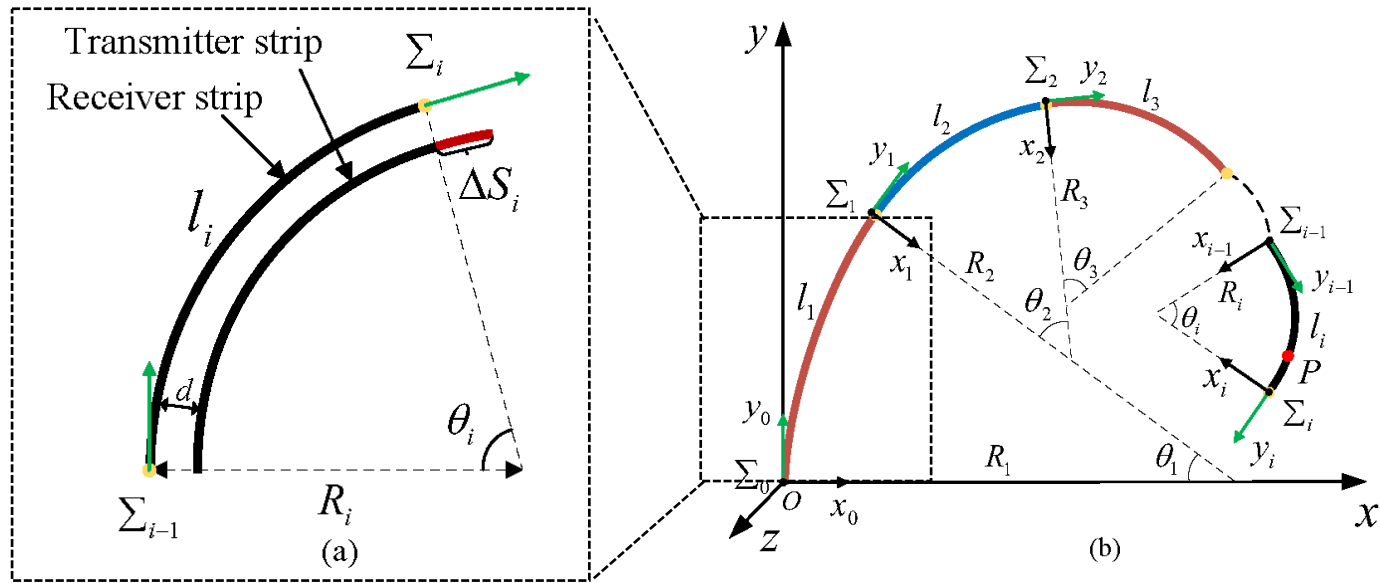


Figure: Assembling with soft fiber-reinforced pneumatic bending actuator (SFPBA)

Shape Reconstruction Algorithm

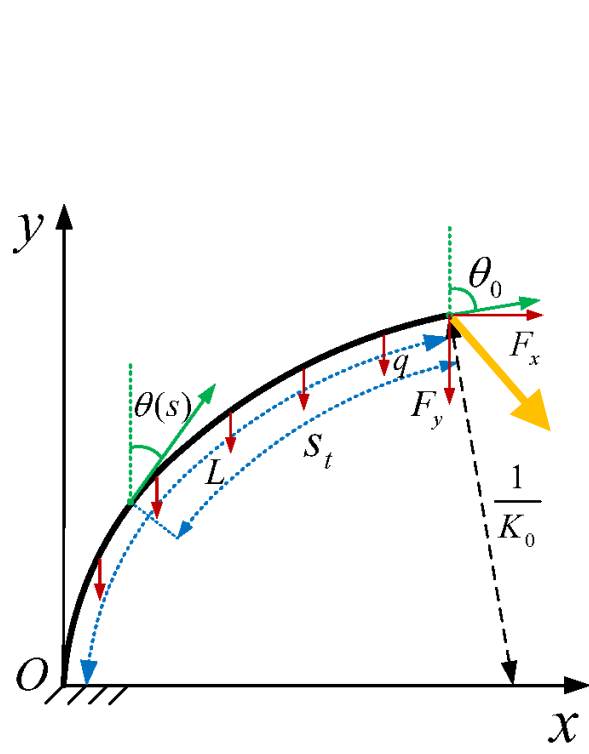


□ P in the inertial frame Σ_0 :

$$\begin{bmatrix} p^0(s) \\ 1 \end{bmatrix} = T_1^0(\theta_1) \cdot T_2^1(\theta_2) \cdots T_{i-1}^{i-2}(\theta_{i-1}) \cdot \begin{bmatrix} p^{i-1}(s) \\ 1 \end{bmatrix} \quad (1)$$

Modeling of Bending Actuator with External Force

- Euler-Bernoulli beam theory for curved cantilever

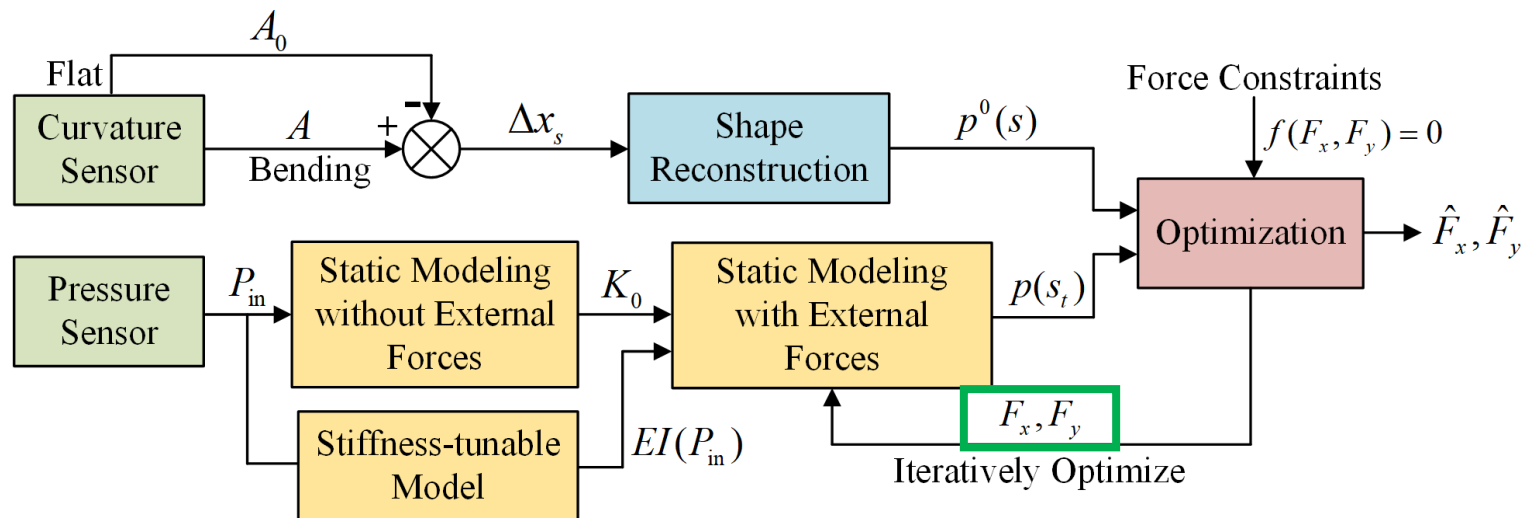


$$\left\{ \begin{array}{l} EI \left(\frac{d^2(\theta(s_t))}{ds_t^2} \right) + F_x \cos(\theta(s_t)) + F_y \sin(\theta(s_t)) + qs_t \sin(\theta(s_t)) = 0 \\ B.C. \quad \theta(L) = 0, \quad \frac{d\theta(0)}{ds_t} = -K_0 \end{array} \right. \quad (4)$$

Integrate for shape:

$$\left\{ \begin{array}{l} x(s_t) = \int_L^{s_t} \sin(\theta(\tau)) d\tau \\ y(s_t) = \int_L^{s_t} \cos(\theta(\tau)) d\tau \\ p(s_t) = [x(s_t) \quad y(s_t) \quad 0]^T \end{array} \right. \quad (5)$$

Force Estimation Algorithm

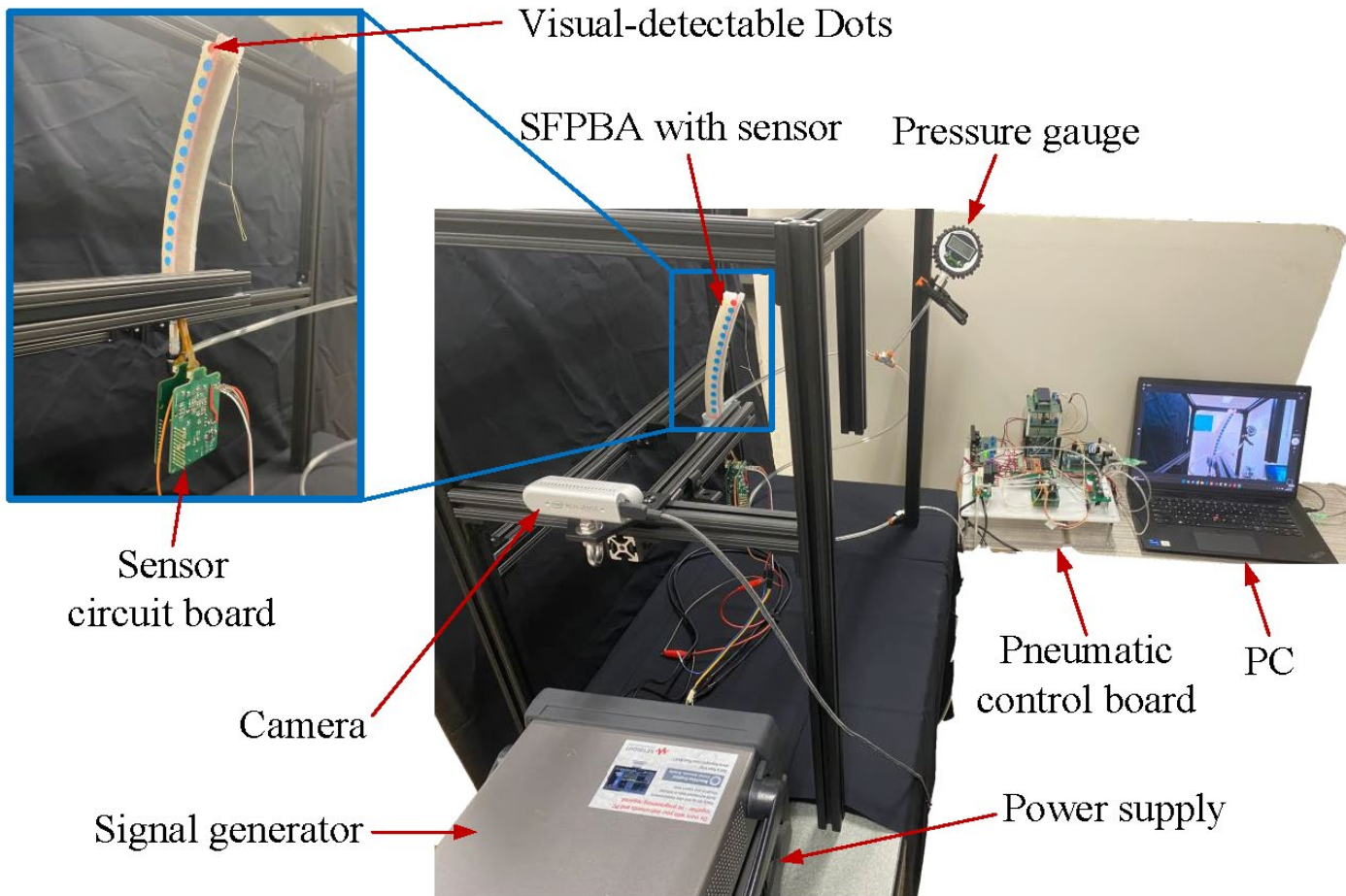


□ Model-based optimization:

$$\begin{aligned}
 (\hat{F}_x, \hat{F}_y) &= \arg \min_{F_x, F_y} \int_0^L \left(\|p^0(s) - p(s_t)\| \right)^2 ds, \\
 \text{s.t. } f(F_x, F_y) &= 0
 \end{aligned} \tag{6}$$

where $f(F_x, F_y) = 0$ captures constraints for practical application (Payload/Contact)

Experimental Setup

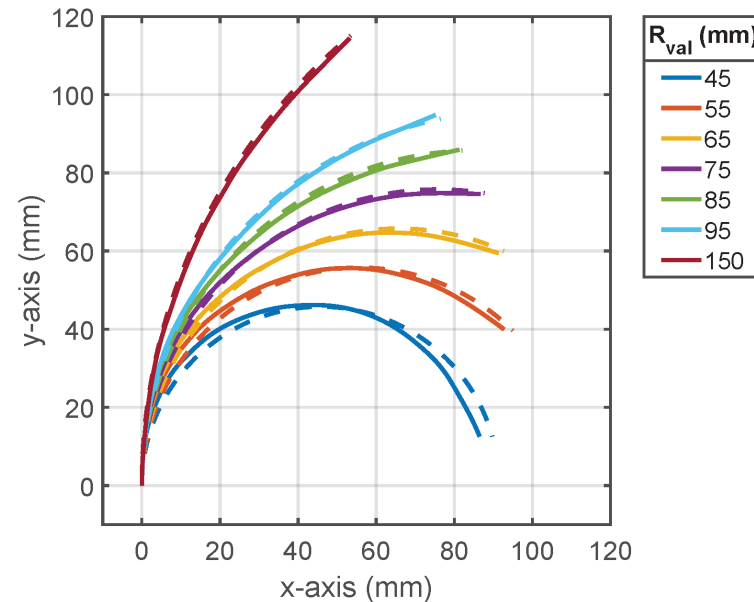
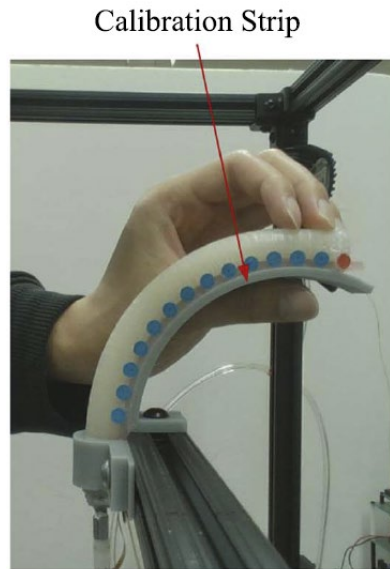


Results on Shape Reconstruction

□ Calibration for Voltage-Shift-Curvature Mapping

$$\delta K = 0.65\% \pm 0.58\%$$

$$(\delta p)_{\max} = 1.59\% \pm 0.72\%$$

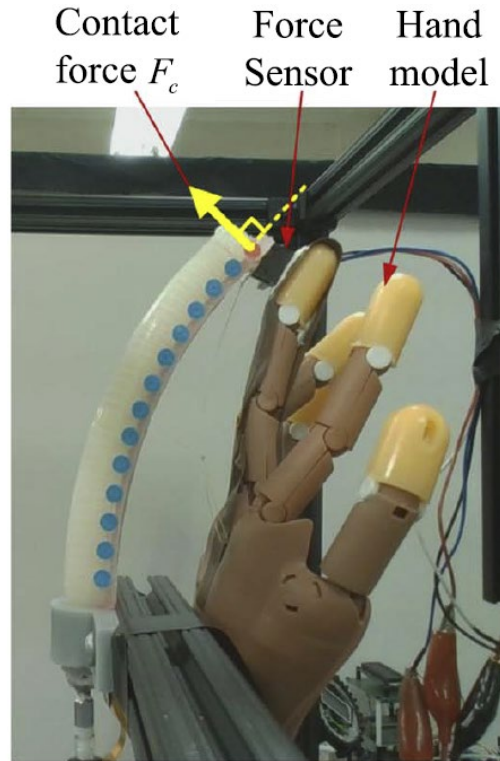


□ Real-time at a minimum frequency of 35 Hz

Demonstration on Shape Reconstruction



Results on Contact Force Estimation



- Constraints: $f(F_x, F_y) = F_x \sin(\theta_0) + F_y \cos(\theta_0) = 0$

Demonstration on Contact Force



Results on Contact Force Estimation

□ Contact force estimation error

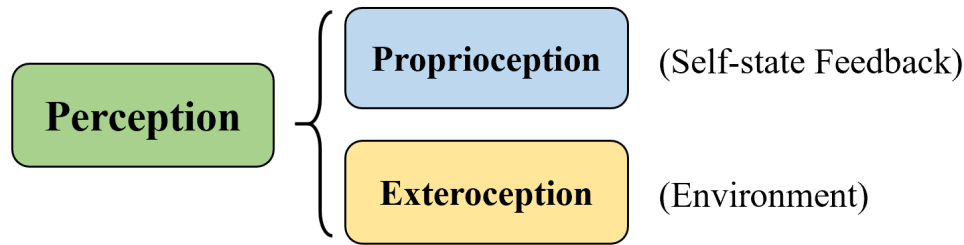
TABLE II
COMPARISON OF MEAN ERRORS (%) IN CONTACT FORCE ESTIMATION WITH
AND WITHOUT GEOMETRIC CONSTRAINT

Force Range (N)	Without Constraint			With Constraint		
	\hat{F}_x	\hat{F}_y	\hat{F}_c	\hat{F}_x	\hat{F}_y	\hat{F}_c
0–0.1	4.13	2.93	4.27	1.57	3.91	2.61
0.1–0.2	8.13	2.51	4.40	3.02	3.43	1.35
0.2–0.3	17.70	13.18	9.04	7.42	4.29	7.52
0.3–0.4	6.29	42.95	12.19	9.15	21.01	8.17
Mean of Full Range	14.90	12.91	7.21	5.15	6.77	4.86

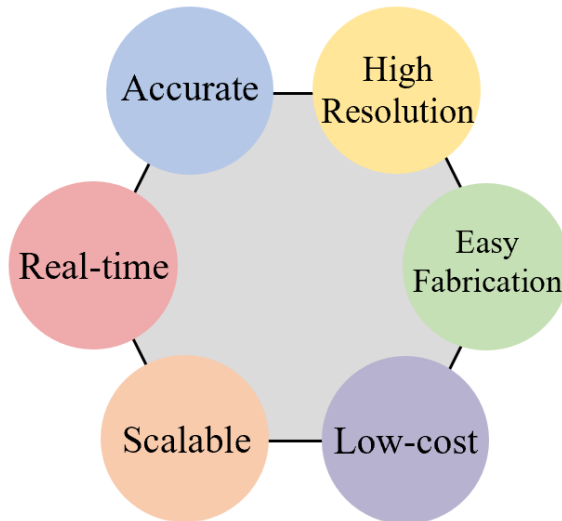
□ Package into integrated App using Matlab *App Designer*

Conclusion

A high-fidelity perception system for soft robots



- ❑ A novel distributed inductive curvature sensor



- ❑ Efficient model-based force estimation

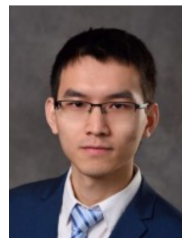
Future Work

1. Develop control algorithms based on continuous shape feedback
2. 3D shape extension

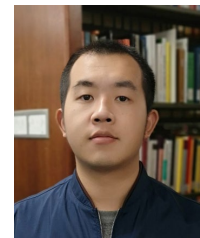
Acknowledgements:



Lei Peng



Dr. Hongyang Shi



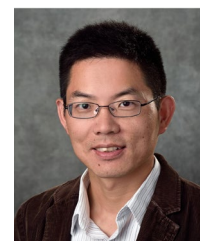
Xinda Qi



Dr. Yiming Deng



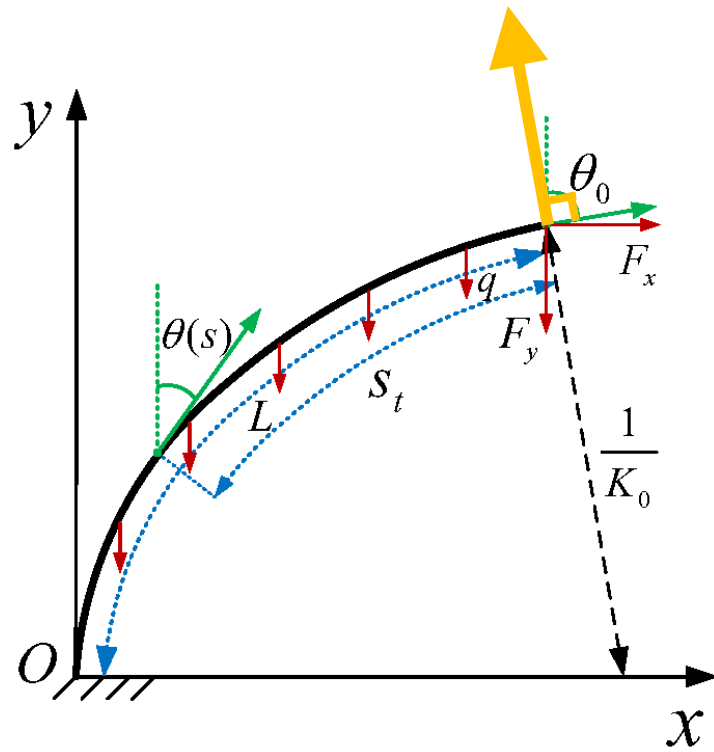
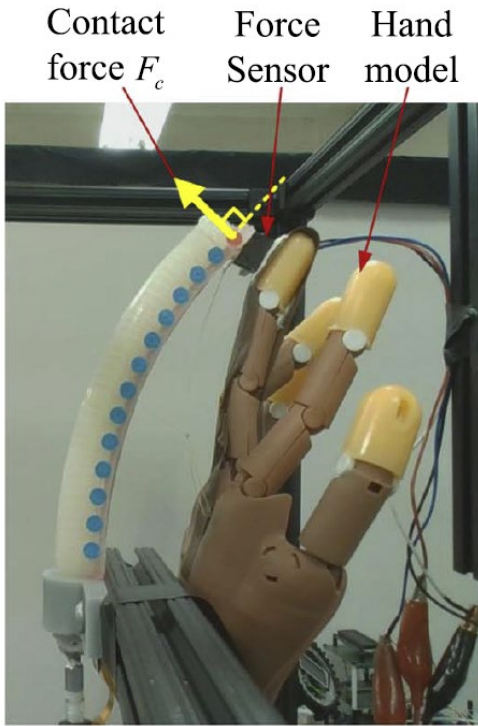
Dr. Vaibhav Srivastava Dr. Xiaobo Tan



This research was supported in part by National Science Foundation awards CMMI 1940950 and CNS 2237577.

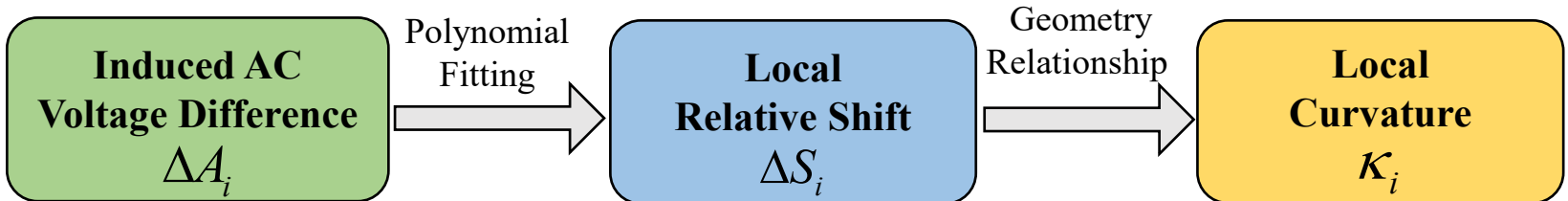
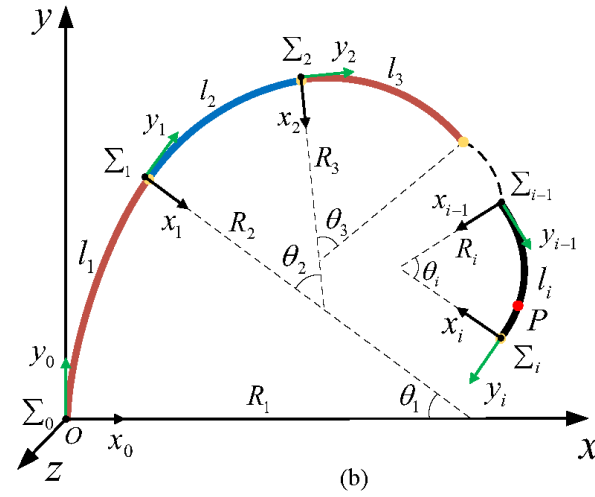
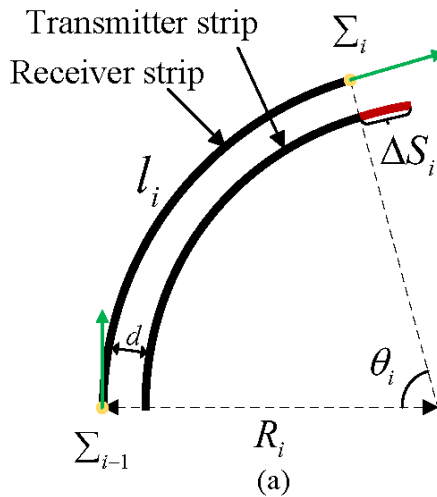


Results on Contact Force Estimation



- Constraints: $f(F_x, F_y) = F_x \sin(\theta_0) + F_y \cos(\theta_0) = 0$

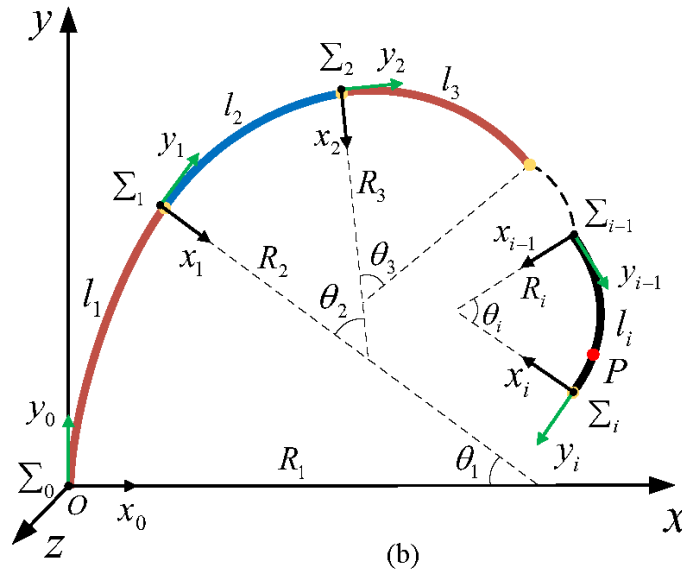
Shape Reconstruction Algorithm



□ Voltage-Shift-Curvature Mapping:

$$S_i = \begin{cases} f_{\text{odd}}(\Delta A_i) = \sum_{k=0}^n a_k (\Delta A_i)^k, & i \text{ is odd,} \\ f_{\text{even}}(\Delta A_i) = \sum_{k=0}^n b_k (\Delta A_i)^k, & i \text{ is even,} \end{cases} \quad \& \quad \kappa_i = \frac{\Delta S_i}{d l_i} \quad (1)$$

Shape Reconstruction Algorithm



(b)

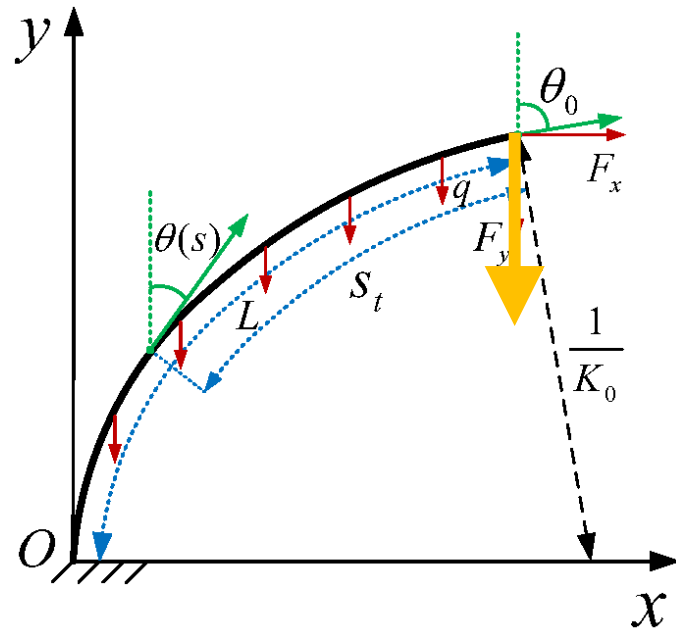
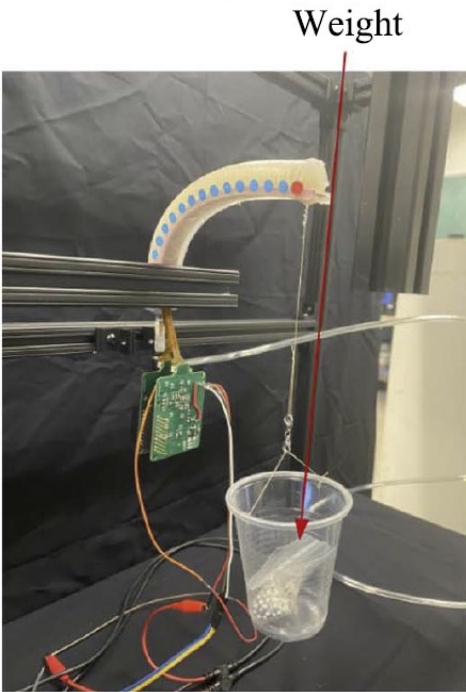
- The homogeneous transformation matrix mapping from Σ_{i-1} to Σ_i :

$$T_i^{i-1}(\theta_i) = \begin{bmatrix} R_z(-\theta_i) & p_i^{i-1}(\theta_i) \\ 0 & 1 \end{bmatrix} \quad (2)$$

- P in the inertial frame Σ_0 :

$$\begin{bmatrix} p^0(s) \\ 1 \end{bmatrix} = T_1^0(\theta_1) \cdot T_2^1(\theta_2) \cdots T_{i-1}^{i-2}(\theta_{i-1}) \cdot \begin{bmatrix} p^{i-1}(s) \\ 1 \end{bmatrix} \quad (3)$$

Results on Tip Load Estimation



- Constraints: $f(F_x, F_y) = F_x = 0$

Demonstration on Tip Loads



- Tip loads estimation error:
 - $0 \sim 0.3N$ 11.9%
 - $0 \sim 0.2N$ 5.49%